

Thermolysis Reactions of *cis*-PtR(SiPh₃)(PMe₂Ph)₂ in Solution

Koh Hasebe, Jun Kamite, Takuya Mori, Hiroyuki Katayama, and
Fumiyuki Ozawa*

Department of Applied Chemistry, Faculty of Engineering, Osaka City University,
Sumiyoshi-ku, Osaka 558-8585, Japan

Received January 7, 2000

A series of *trans*- and *cis*-PtR(SiPh₃)(PMe₂Ph)₂ complexes have been prepared and their thermolysis reactions in solution examined. The *trans* isomers (R = Me, Et) are robust, and only the methyl complex affords MeSiPh₃ as the reductive elimination product in 72–82% yields. In contrast, the *cis* isomers (R = Me, Et, Pr, Bu) form the corresponding alkylsilanes in almost quantitative yields (>97%). Despite the selective formation of the reductive elimination products, the *cis*-alkyl–silyl complexes bearing β -hydrogens undergo a rapid repetition of the β -hydrogen elimination and insertion processes, as confirmed by a deuterium-labeling experiment using *cis*-Pt(CH₂CD₃)(SiPh₃)(PMe₂Ph)₂. The alkylsilane formation from the *cis* isomers proceeds via two reaction paths. One is the direct C–Si reductive elimination. On the other path, the *cis*-PtR(SiPh₃)(PMe₂Ph)₂ complexes are initially isomerized to the corresponding *cis*-PtPh(SiRPh₂)(PMe₂Ph)₂ complexes by the exchange of the Pt–R group with the Si–Ph group, and the resulting phenyl–silyl complexes reductively eliminate alkylsilanes. The methyl–silyl complex decomposes exclusively by the former path, while the other alkyl–silyl complexes (R = Et, Pr, Bu) follow mainly the latter path. Preparation and thermolysis reaction of the related *cis*-PtEt(GePh₃)(PMe₂Ph)₂ are also reported.

Introduction

While the C–Si bond formation from alkyl(silyl)-platinum complexes is the most widely accepted product-forming step for platinum-catalyzed hydrosilylation of alkenes,^{1,2} little is known about this elementary process.^{3–5} We recently reported that *cis*-PtMe(SiPh₃)-L₂ complexes (L = PMePh₂, PMe₂Ph) readily afford MeSiPh₃ in quantitative yields in solution.^{6,7} This

reaction is effectively accelerated by alkynes and alkenes added to the systems, particularly by those with electron-withdrawing substituents. Kinetic studies indicated that the MeSiPh₃ formation in the presence of diphenylacetylene proceeds via the mechanism involving prior replacement of one of the phosphine ligands (L) with diphenylacetylene, followed by reductive elimination of MeSiPh₃ from the resulting [PtMe(SiPh₃)-(PhC≡CPh)(L)] intermediate.

To gain further insights into the C–Si bond formation from a platinum(II) center, we prepared in this study a series of *cis*-PtR(SiPh₃)(PMe₂Ph)₂ complexes bearing R groups with β -hydrogens (i.e., Et, Pr, Bu) and examined their thermolysis reactions in solution. While the reactivity was much lower than that of *cis*-PtMe(SiPh₃)(PMe₂Ph)₂, the alkyl–silyl complexes exclusively afforded alkylsilanes as the C–Si reductive elimination products. In addition, the alkylsilane formation was found to take place mainly from *cis*-PtPh(SiRPh₂)(PMe₂Ph)₂ intermediates, which are formed by the exchange of the Pt–R group with the Si–Ph group. Related studies on the thermolysis of *trans*-PtR(SiPh₃)(PMe₂Ph)₂ (R = Me, Et) and *cis*-PtEt(GePh₃)(PMe₂Ph)₂ are also reported.

Results and Discussion

Preparation of *trans*- and *cis*-PtR(SiPh₃)(PMe₂Ph)₂. The alkyl–silyl complexes (**1** and **2**) employed in this study are listed in Chart 1. Complexes **1a**, **1b**, **2a**, and **2b** were prepared previously.^{7,8} The propyl and butyl complexes (**2c** and **2d**) were synthesized similarly

(1) (a) Hiyama, T.; Kusumoto, T. In *Comprehensive Organic Synthesis*; Trost, B. M., Fleming, I., Eds.; Pergamon Press: Oxford, 1991; Vol. 8, p 763. (b) Ojima, I. In *The Chemistry of Organic Silicon Compounds*; Patai, S., Rappoport, Z., Eds.; John Wiley: Chichester, 1989; p 1479. (c) Braustein, P.; Knorr, M. *J. Organomet. Chem.* **1995**, *500*, 21. (d) Recatto, C. A. *Aldrichim. Acta* **1995**, *28*, 85. (e) Tilley, T. D. In *The Chemistry of Organic Silicon Compounds*; Patai, S., Rappoport, Z., Eds.; John Wiley: Chichester, 1989; p 1415.

(2) (a) Chalk, A. J.; Harrod, J. F. *J. Am. Chem. Soc.* **1965**, *87*, 16. (b) Harrod, J. F.; Chalk, A. J. *J. Am. Chem. Soc.* **1965**, *87*, 1133. (c) Stein, J.; Lewis, L. N.; Gao, Y.; Scott, R. A. *J. Am. Chem. Soc.* **1999**, *121*, 3693, and references therein.

(3) van der Boom, M. E.; Ott, J.; Milstein, D. *Organometallics* **1998**, *17*, 4263.

(4) Sakaki, S.; Mizoe, N.; Sugimoto, M. *Organometallics* **1998**, *17*, 2510.

(5) For related studies other than platinum systems, see: (a) Maruyama, Y.; Yamamura, K.; Ozawa, F. *Chem. Lett.* **1998**, 905. (b) Tanaka, Y.; Yamashita, H.; Shimada, S.; Tanaka, M. *Organometallics* **1997**, *16*, 3246. (c) Akita, M.; Hua, R.; Oku, T.; Tanaka, M.; Moro-oka, Y. *Organometallics* **1996**, *15*, 4162. (d) Okazaki, M.; Tobita, H.; Ogino, H. *Organometallics* **1996**, *15*, 2790. (e) Mitchell, G. P.; Tilley, T. D. *Organometallics* **1996**, *15*, 3477. (f) Aizenberg, M.; Milstein, D. *J. Am. Chem. Soc.* **1995**, *117*, 6456. (g) Schubert, U. *Angew. Chem., Int. Ed. Engl.* **1994**, *33*, 419. (h) Lin, W.; Wilson, S. R.; Girolami, G. S. *Organometallics* **1994**, *13*, 2309. (i) Schubert, U.; Müller, C. *J. Organomet. Chem.* **1989**, *373*, 165. (j) Brinkman, K. C.; Blakeney, A. J.; Krone-Schmidt, W.; Gladysz, J. A. *Organometallics* **1984**, *3*, 1325.

(6) Ozawa, F.; Hikida, T.; Hayashi, T. *J. Am. Chem. Soc.* **1994**, *116*, 2844.

(7) Ozawa, F.; Hikida, T.; Hasebe, K.; Mori, T. *Organometallics* **1998**, *17*, 1018.

(8) Ozawa, F.; Hikida, T. *Organometallics* **1996**, *15*, 4501.

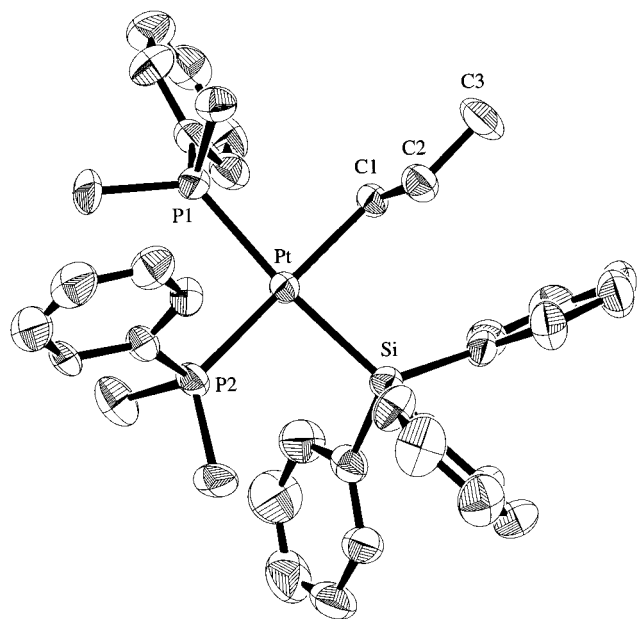
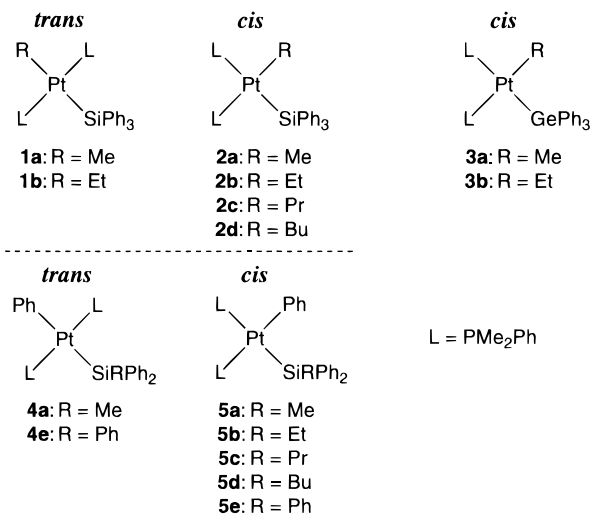


Figure 1. Molecular structure of *cis*-Pt(*n*-Pr)(SiPh₃)(PMe₂Ph)₂ (**2c**). Thermal ellipsoids are drawn at the 50% probability level. Selected bond distances (Å) and angles (deg): Pt–P(1) = 2.358(2), Pt–P(2) = 2.304(2), Pt–Si = 2.367(2), Pt–C(1) = 2.128(8), P(1)–Pt–P(2) = 94.75(8), P(1)–Pt–Si = 169.5(1), P(1)–Pt–C(1) = 85.5(2), P(2)–Pt–Si = 93.6(1), P(2)–Pt–C(1) = 172.9(2), Si–Pt–C(1) = 87.0(2).

Chart 1



to **2a** and **2b**. Thus, the treatment of *trans*-PtCl(SiPh₃)(PMe₂Ph)₂ with an excess amount of RLi (R = Pr or Bu) in THF at 0 °C gave a platinate complex Li[PtR₂(SiPh₃)(PMe₂Ph)] with liberation of 1 equiv of PMe₂Ph. Methanolysis of the reaction mixture at –30 °C formed the alkyl–silyl complex.

Complexes **2c** and **2d** were isolated as white crystalline solids and identified by NMR spectroscopy and elemental analysis. Complex **2c** was also examined by single-crystal X-ray diffraction analysis. Figure 1 shows an ORTEP diagram. The platinum atom has a slightly distorted square planar geometry; the sum of four angles about platinum is 360.85°. The propyl group is extruded linearly from the platinum center. The P(2)–Pt–Si angle (93.6(1)°) is much wider than the P(1)–Pt–C(1) angle (85.5(2)°), probably reflecting the bulki-

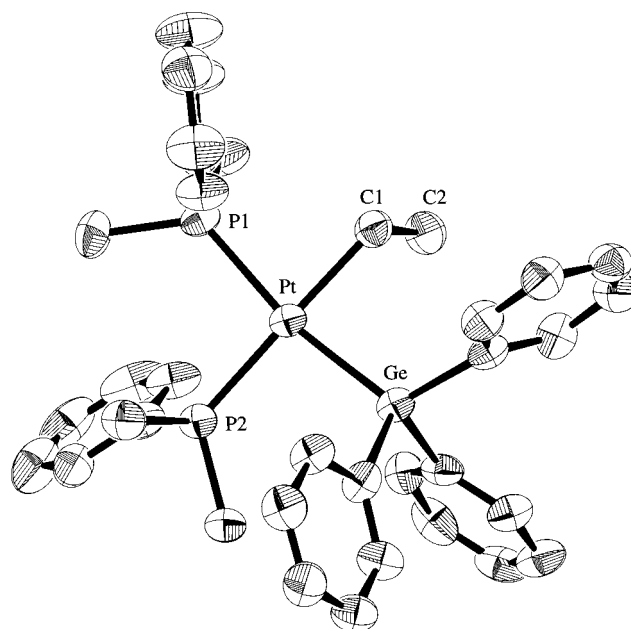


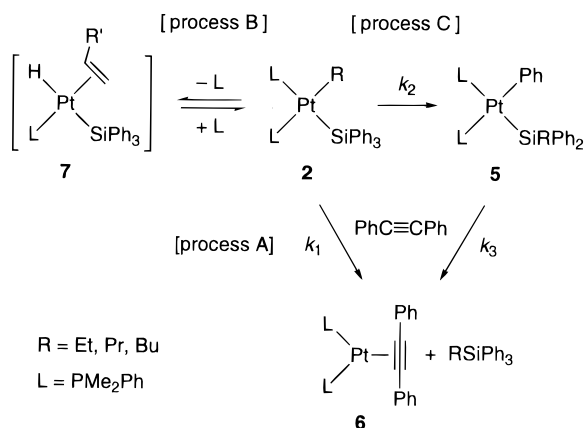
Figure 2. Molecular structure of *cis*-PtEt(GePh₃)(PMe₂Ph)₂ (**3b**). Thermal ellipsoids are drawn at the 50% probability level. Selected bond distances (Å) and angles (deg): Pt–Ge = 2.437(1), Pt–P(1) = 2.307(2), Pt–P(2) = 2.311(2), Pt–C(1) = 2.134(9), Ge–Pt–P(1) = 166.50(6), Ge–Pt–P(2) = 94.35(5), Ge–Pt–C(1) = 85.6(2), P(1)–Pt–P(2) = 96.76(8), P(1)–Pt–C(1) = 84.1(2), P(2)–Pt–C(1) = 174.8(2).

ness of the SiPh₃ ligand. The Pt–P(1) bond (2.358(2) Å) is longer than the Pt–P(2) bond (2.304(2) Å), owing to the higher trans influence of the SiPh₃ ligand than the Pr ligand. However, the difference between the two Pt–P distances in **2c** (0.054 Å) was much smaller than that observed for *cis*-PtMe(SiPh₃)(PMePh₂)₂ (0.268 Å).⁶ This is mainly due to the higher trans influence of the Pr ligand than the Me ligand. Actually, the ¹J_{Pt–P(2)} value of **2c** (1783 Hz) was significantly smaller than that of **2a** (2048 Hz)⁸ and *cis*-PtMe(SiPh₃)(PMePh₂)₂ (2136 Hz).⁶

Preparation of *cis*-PtEt(GePh₃)(PMe₂Ph)₂. The title compound (**3b**) was synthesized by the reaction of *trans*-PtCl(GePh₃)(PMe₂Ph)₂ with EtLi in THF at 0 °C, followed by methanolysis of the reaction mixture at –30 °C. The X-ray structure is given in Figure 2. The geometry around the platinum is very similar to that of *cis*-PtMe(GePh₃)(PMe₂Ph)₂ (**3a**).⁷ Thus, the platinum atom is in a slightly distorted square planar environment, and the Ge–Pt–P(2) angle is much wider than the P(1)–Pt–C(1) angle. The Pt–Ge bond (2.437(1) Å) is somewhat shorter than that of **3a** (2.4495(7) Å), while the Pt–C(1) bond (2.134(9) Å) is longer than that of **3a** (2.127(5) Å). The Pt–P(1) and Pt–P(2) bond distances in **3b** are almost identical with each other (2.31 Å). This fact differs from **3a**, in which the Pt–P bond trans to the GePh₃ ligand (2.330(1) Å) is somewhat longer than the Pt–P bond trans to the Me ligand (2.308(2) Å).

Thermolysis Products. The alkyl–silyl and alkyl–germyl complexes thus prepared were subjected to thermolysis in benzene-*d*₆ or toluene-*d*₈ in the presence of an excess amount of diphenylacetylene, which was added to facilitate the reductive elimination and to trap platinum(0) species generated in the systems as Pt(PhC≡CPh)(PMe₂Ph)₂ (**6**).^{6,7} The reaction progress was

Scheme 1



followed by $^{31}\text{P}\{^1\text{H}\}$ NMR spectroscopy, and the organic products were analyzed by GLC and GC–mass spectrometry.

The *trans*-methyl-silyl complex (**1a**) decomposed mainly by a reductive elimination process. The reaction examined in toluene- d_8 in the presence of diphenylacetylene (40 equiv) was completed for 45 h at 70 °C, yielding MeSiPh_3 in 72%. In the presence of $\text{MeO}_2\text{C}-\text{C}\equiv\text{CCO}_2\text{Me}$ (40 equiv) in place of diphenylacetylene, the C–Si reductive elimination took place under much milder conditions (35 °C, 2.5 h) to give MeSiPh_3 in 82% yield. The *trans*-ethyl-silyl complex (**1b**) also decomposed under heated conditions (>60 °C), but only small amounts of EtSiPh_3 (<2%) and HSiPh_3 (<4%) were observed in the reaction solution; no other product was detected by GC–mass spectrometry.

Unlike the *trans* complexes, *cis*-alkyl-silyl complexes (**2a–2d**) afforded the reductive elimination products (RSiPh_3) in almost quantitative yields (>97%) irrespective of the alkyl ligands. The reaction of **2a** proceeded even at room temperature, while **2b–2d** were more stable and decomposed under heated conditions (>35 °C).

The *cis*-ethyl-germyl complex (**3b**) was extremely stable toward reductive elimination, and no trace of EtGePh_3 was formed by the thermolysis in toluene- d_8 at 90 °C. The high stability of the alkyl-germyl complex, as compared with alkyl-silyl analogues, has already been observed for *cis*- $\text{PtMe}(\text{GePh}_3)(\text{PMe}_2\text{Ph})_2$ (**3b**).⁷

Thermolysis Processes of *cis*- $\text{PtR}(\text{SiPh}_3)(\text{PMe}_2\text{Ph})_2$. While **2b–2d** gave the corresponding alkylsilanes as the reductive elimination products in almost quantitative yields, the thermolysis reactions were found to involve two additional processes (Scheme 1). One is reversible β -hydrogen elimination from the alkyl ligand (process B), and the other is isomerization of *cis*- $\text{PtR}(\text{SiPh}_3)(\text{PMe}_2\text{Ph})_2$ to *cis*- $\text{PtPh}(\text{SiRPh}_2)(\text{PMe}_2\text{Ph})_2$ (process C).

The occurrence of process B was confirmed by thermolysis experiments using a deuterium-labeled complex *cis*- $\text{Pt}(\text{CH}_2\text{CD}_3)(\text{SiPh}_3)(\text{PMe}_2\text{Ph})_2$ (**2b-d₃**). Heating a mixture of **2b-d₃** and diphenylacetylene (10 equiv) in benzene- d_6 at 40 °C overnight led to the formation of EtSiPh_3 in 98% yield, as confirmed by GLC using MeSiPh_3 as an internal standard. The ^2D NMR spectrum of the resulting solution exhibited two signals assignable to the methyl and methylene groups of

EtSiPh_3 (δ 1.08 and 1.28, respectively) in a 3.1:1.9 ratio, the value of which was close to the ratio expected for the random H–D scrambling in these two groups (3.0:2.0).

The EtSiPh_3 formation involving a reversible β -hydrogen elimination process can be rationalized by assuming a rapid equilibrium between **2b** and a hydridosilyl ethylene complex **7** ($\text{R}' = \text{H}$) under thermolysis conditions (Scheme 1). As previously demonstrated for *cis*- $\text{PtEt}_2(\text{PPh}_3)_2$,⁹ the β -hydrogen elimination very probably involves prior dissociation of the phosphine ligand *cis* to the ethyl ligand, giving **7**, having the hydrido and SiPh_3 ligands in mutually *trans* positions. Owing to this geometry, **7** is unable to undergo H–Si reductive elimination. Therefore, the thermolysis of **2b** exclusively forms the C–Si reductive elimination product, despite the occurrence of rapid β -hydrogen elimination.

On the other hand, the participation of process C in the thermolysis reaction was indicated by NMR spectroscopy. Figure 3 shows a typical $^{31}\text{P}\{^1\text{H}\}$ NMR spectrum of the thermolysis solution of **2c** in benzene- d_6 at 55 °C in the presence of diphenylacetylene (10 equiv). Besides the signals due to **2c** (δ –5.2 and –12.5) and the reductive elimination product $\text{Pt}(\text{PhC}\equiv\text{CPh})(\text{PMe}_2\text{Ph})_2$ (**6**) (δ –13.0), two sets of doublets are observed at δ –6.2 and –14.1 in a 1:1 ratio. As described in the following section, these signals are assigned to *cis*- $\text{PtPh}(\text{SiPrPh}_2)(\text{PMe}_2\text{Ph})_2$ (**5c**), formed by the exchange of the Pt–Pr group with the Si–Ph group in **2c**. Similarly, the formation of *cis*- $\text{PtPh}(\text{SiEtPh}_2)(\text{PMe}_2\text{Ph})_2$ (**5b**) [δ –6.4 (d, $^2J_{\text{P-P}} = 19$ Hz, $^1J_{\text{Pt-P}} = 1133$ Hz), –14.4 (d, $^2J_{\text{P-P}} = 19$ Hz, $^1J_{\text{Pt-P}} = 1953$ Hz)] and *cis*- $\text{PtPh}(\text{SiBuPh}_2)(\text{PMe}_2\text{Ph})_2$ (**5d**) [δ –6.7 (d, $^2J_{\text{P-P}} = 18$ Hz, $^1J_{\text{Pt-P}} = 1130$ Hz), –14.6 (d, $^2J_{\text{P-P}} = 18$ Hz, $^1J_{\text{Pt-P}} = 1950$ Hz)] was found in the thermolysis solutions of **2b** and **2d**, respectively.

Figure 4 shows the change of platinum complexes with time in the thermolysis solution of **2b**. On heating the sample solution at 50 °C, **5b** and **6** simultaneously appeared at the expense of **2b**. The amount of **5b** reached a maximum (17%) after ca. 60 min and then gradually decreased, while the amount of diphenylacetylene complex **6** increased further. Finally, **2b** and **5b** disappeared, and only the signal of **6** was observed in the $^{31}\text{P}\{^1\text{H}\}$ NMR spectrum.

The time-course in Figure 4 corresponds to the consecutive reaction path (**2b** → **5b** → **6**) in Scheme 1 ($\text{R} = \text{Et}$). However, detailed analysis of the reaction curves indicated the concurrent operation of a direct path from **2b** to **6** (process A) as well. Thus, the dot lines in this figure show ideal reaction curves for the stepwise conversion of **2b** to **6** via **5b** with the rate constants $k_2 = 1.4 \times 10^{-4} \text{ s}^{-1}$ and $k_3 = 2.6 \times 10^{-4} \text{ s}^{-1}$ ($k_1 = 0.0 \text{ s}^{-1}$). It is seen that the calculated curve for **6** is clearly S-shaped, showing a slow formation of **6** at the initial stage, while the amount of **6** increases linearly from the beginning in reality. This fact strongly indicates the concomitance of the direct path from **2b** to **6**. Actually, the experimental data are in good agreement with the solid lines, which are calculated for the parallel formation of **6** via processes A and C: $k_1 = 6.0 \times 10^{-5} \text{ s}^{-1}$, $k_2 = 8.0 \times 10^{-5} \text{ s}^{-1}$, $k_3 = 2.1 \times 10^{-4} \text{ s}^{-1}$.¹⁰

(9) (a) McCarthy, T. J.; Nuzzo, R. G.; Whitesides, G. M. *J. Am. Chem. Soc.* **1981**, *103*, 1676 and 3396. (b) Komiya, S.; Morimoto, Y.; Yamamoto, A.; Yamamoto, T. *Organometallics* **1982**, *1*, 1528.

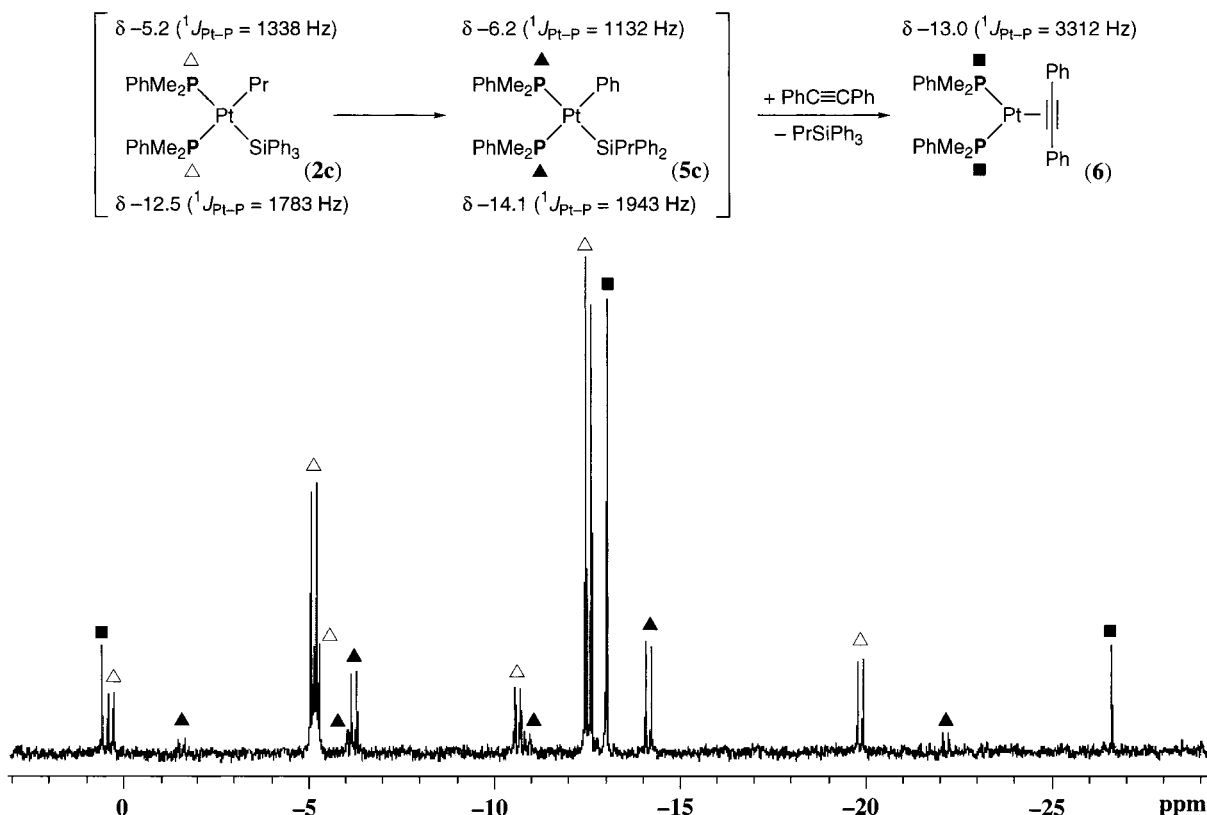


Figure 3. $^{31}\text{P}\{^1\text{H}\}$ NMR spectrum (121.48 MHz) of the thermolysis solution of **2c** in benzene- d_6 in the presence of diphenylacetylene (10 equiv) at 55 °C.

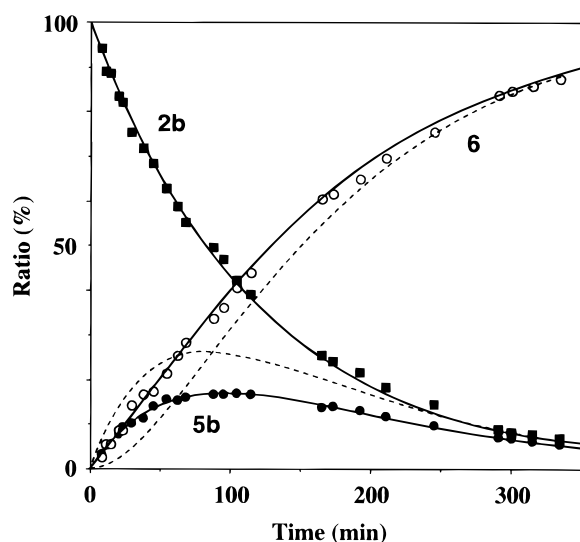


Figure 4. Time-course of the thermolysis of **2b** in benzene- d_6 at 50 °C in the presence of diphenylacetylene: $[\mathbf{2b}]_0 = 20$ mM, $[\text{PhC}\equiv\text{CPh}]_0 = 0.20$ M. The solid and dotted lines exhibit calculated reaction curves (see text).

Table 1 summarizes the rate constants for the thermolysis of **2b**, **2c**, and **2d** in benzene- d_6 at 55 °C in the presence of diphenylacetylene (0.20 M, 10 equiv). Also listed is the rate constant for the reductive elimination

Table 1. Rate Constants for the Thermolysis of **2b–2d** (Scheme 1) at 55 °C in Benzene- d_6 in the Presence of Diphenylacetylene^a

complex	rate constant ($10^4 k, \text{s}^{-1}$)
2b (R = Et)	$k_1 = 1.0$ $k_2 = 1.5$ ($k_1 + k_2 = 2.5$) $k_3 = 3.5$
2c (R = Pr)	$k_1 = 0.61$ $k_2 = 1.0$ ($k_1 + k_2 = 1.6$) $k_3 = 1.8$
2d (R = Bu)	$k_1 = 0.58$ $k_2 = 0.81$ ($k_1 + k_2 = 1.4$) $k_3 = 1.4$
2a (R = Me) (toluene- d_8)	$k_1 = 33^b$

^a Initial concentration: $[\text{complex}]_0 = 20$ mM, $[\text{PhC}\equiv\text{CPh}] = 0.20$ M. ^b The value was extrapolated from an Eyring plot at 20–45 °C (see ref 7).

from **2a** (k_1). The k_2 value is about 1.5 times larger than the k_1 value for all systems, showing the predominant operation of the consecutive reaction path (**2** → **5** → **6**) in Scheme 1. The rate constants for the direct formation of **6** (k_1), which decrease in the order **2b** > **2c** ≥ **2d**, are much smaller than that of **2a**.

Identification of *cis*-PtPh(SiRPh₂)(PMe₂Ph)₂. The conversion of **2b–2d** into **5b–5d**, respectively (process C in Scheme 1), could be observed in over 80% selectivities, when the reactions were performed in CD₂Cl₂ at room temperature in the absence of diphenylacetylene as a promoter of the C–Si reductive elimination. The isomerization was a significantly slow process, taking a few days for completion. Although **5b–5d** could not be isolated from the reaction solutions due to contami-

(10) The calculation was performed with the following rate expressions: $-d[\mathbf{2}]/dt = (k_1 + k_2)[\mathbf{2}]$; $d[\mathbf{5}]/dt = k_2[\mathbf{2}] - k_3[\mathbf{5}]$; $d[\mathbf{6}]/dt = k_1[\mathbf{2}] + k_3[\mathbf{5}]$. The rate constants k_2 and k_3 include terms of $[\text{PhC}\equiv\text{CPh}]$, as confirmed for the formation of MeSiPh₃ from **2a**.⁷ The amount of each component at time t is given as follows. $[\mathbf{2}] = [\mathbf{2}]_0 \exp(-(k_1 + k_2)t)$. $[\mathbf{5}] = [\mathbf{2}]_0 \{k_2/(k_3 - k_1 - k_2)\} \{\exp(-(k_1 + k_2)t) - \exp(-k_3t)\}$. $[\mathbf{6}] = [\mathbf{2}]_0 - [\mathbf{5}]$.

Table 2. Characteristic NMR Data of *cis*-PtPh(SiRPh₂)(PMe₂Ph)₂^a

complex (R)	¹ H NMR				³¹ P{ ¹ H} NMR			
	δ	² J _{P-H}	³ J _{Pt-H}	assignment	δ	² J _{P-P}	¹ J _{Pt-P}	² J _{Si-P}
5b (Et)	0.90 (d)	7.2	15.6	PMe	−14.6 (d)	19	1948	
	1.00 (d)	8.4	19.2	PMe	−6.1 (d)	19	1160	174
	6.72 (brt)			<i>p</i> -Ph				
	6.88 (brt)			<i>m</i> -Ph				
5c (Pr)	0.91 (d)	7.6	16.0	PMe	−14.8 (d)	19	1949	
	1.04 (d)	8.0	22.4	PMe	−6.1 (d)	19	1188	182
	6.68 (brt)			<i>p</i> -Ph				
	6.84 (brt)			<i>m</i> -Ph				
5d (Bu)	0.91 (d)	7.6	17.6	PMe	−14.8 (d)	18	1949	
	1.03 (d)	8.4	21.6	PMe	−6.2 (d)	18	1184	182
	6.67 (brt)			<i>p</i> -Ph				
	6.82 (brt)			<i>m</i> -Ph				
5a (Me)	0.94 (d)	7.6	16.8	PMe	−14.8 (d)	19	1936	
	1.03 (d)	8.4	22.4	PMe	−5.6 (d)	19	1240	178
	6.67 (brt)			<i>p</i> -Ph				
	6.85 (brt)			<i>m</i> -Ph				
5e (Ph)	0.91 (d)	7.8	16.6	PMe	−13.4 (d)	19	1808	
	1.03 (d)	8.3	22.0	PMe	−4.2 (d)	19	1156	183
	6.36 (brt)			<i>p</i> -Ph				
	6.47 (brt)			<i>m</i> -Ph				

^a Solvent: CD₂Cl₂ (**5a**, **5c**, **5d**, **5e**), CDCl₃ (**5b**). Temp (°C): 23 (**5b**, **5c**, **5d**, **5e**), −20 (**5a**).

nation with the starting complexes and some unidentified platinum species, their structures could be unequivocally confirmed by NMR spectroscopy.

Table 2 lists the characteristic NMR data of **5b–5d**. Also included for comparison are data of the related phenyl–silyl complexes **5a** and **5e**, which were isolated and fully characterized by NMR spectroscopy and elemental analysis (see Experimental Section). The ¹H NMR spectra exhibited two broad triplets assignable to the para and meta protons of the Pt–Ph group at around δ 6.7 and 6.8, which were not observed for *cis*-alkyl–silyl complexes **2a–2d** and characteristic of the phenyl–silyl complexes. The distinct upfield shifts observed for the phenyl protons are attributable to ring-current of the P–Ph and Si–Ph groups, which may be situated near the Pt–Ph group. The ³¹P{¹H} NMR signals were observed as two sets of doublets at around δ −14.8 and −6.1 with relatively large and small ¹J_{Pt-P} values (ca. 1950 and 1180 Hz), respectively. These coupling constants were comparable to those of **5a** and **5e**, but clearly different from those of **2b–2d** (1792–1783 and 1437–1367 Hz).

On the Difference of Thermolysis Processes between Methyl and the Other Alkyl Complexes. We found in this study that the alkylsilane formation from **2b–2d** proceeds mainly via the isomerization of these complexes to *cis*-PtPh(SiRPh₂)(PMe₂Ph)₂ (**5b–5d**) (process C).¹¹ Thus, the isomerization of **2** (*k*₂) and the successive C–Si reductive elimination from **5** (*k*₃) took place about 1.5 and 3 times faster than the direct reductive elimination from **2** (*k*₁), respectively (Table 1). On the other hand, we previously reported that the

methyl–silyl complex **2a** undergoes direct reductive elimination, exclusively.⁷ Although we reexamined the thermolysis solution of **2a** by ³¹P{¹H} NMR spectroscopy, no sign of the formation of *cis*-PtPh(SiMePh₂)(PMe₂Ph)₂ (**5a**) was detected. It was further confirmed that the C–Si reductive elimination from **2a** (*k*₁ = 1.2 × 10^{−3} s^{−1} at 45 °C in toluene-*d*₈ in the presence of diphenylacetylene (0.20 M)) is about 8 times faster than the MeSiPh₃ formation from **5a** (*k*₃ = 1.5 × 10^{−4} s^{−1} at 45 °C in benzene-*d*₆ in the presence of diphenylacetylene (0.20 M)).

The difference of thermolysis paths between **2a** and the other alkyl–silyl complexes **2b–2d** will be attributed to differences in the reactivity of these complexes toward direct reductive elimination. Thus, the *k*₁ value of **2a** was 33–57 times larger than that of **2b–2d** (Table 1). The observed reactivity order for C–Si reductive elimination (R = Me ≫ Et > Pr ≥ Bu) is significant because this order is just the reverse of conventional C–C reductive elimination.¹² This fact implies a unique mechanistic feature of the C–Si reductive elimination and deserves a discussion.

As we already confirmed for the thermolysis of **2a**, the rate of reductive elimination of alkylsilane is controlled at two stages.^{6,7} One is the reversible exchange of the PMe₂Ph ligand trans to the SiPh₃ ligand with diphenylacetylene, and the other is the reductive elimination of alkylsilane from the [PtR(SiPh₃)(PhC≡CPh)(PMe₂Ph)] intermediate. Since the former stage may be affected mainly by the trans effect of the silyl ligand, the equilibrium constants for **2a–2d** bearing the same SiPh₃ ligand will be very similar to each other. Accordingly, one may consider that the reactivity order observed for the SiPh₃ complex series (**2a** ≫ **2b** > **2c** ≥ **2d**) should be determined at the second stage as the rate-determining step.

(11) (a) Process C is thought to proceed via a silylene intermediate, which is formed by dissociation of a phosphine ligand, followed by α-Ph group elimination from the SiPh₃ ligand. Such a process has been proposed for an iridium system: Burger, P.; Bergman, R. G. *J. Am. Chem. Soc.* **1993**, *115*, 10462. (b) For precedents of platinum silylene complexes, see: Mitchell, G. P.; Tilley, T. D. *Angew. Chem., Int. Ed.* **1998**, *37*, 2524; *J. Am. Chem. Soc.* **1998**, *120*, 7635. (c) The C–Si bond formation via α-migration of an alkyl ligand to a silylene ligand has been proposed: Okazaki, M.; Tobita, H.; Ogino, H. *J. Chem. Soc., Dalton Trans.* **1997**, 3531. Ozawa, F.; Kitaguchi, M.; Katayama, H. *Chem. Lett.* **1999**, 1289. (d) For further information on the related chemistry, see: Peters, J. C.; Feldman, J. D.; Tilley, T. D. *J. Am. Chem. Soc.* **1999**, *121*, 9871, and references therein.

(12) The reactivity toward C–C reductive elimination generally increases as the σ-donating ability of the alkyl ligand increases. (a) Tatsumi, K.; Hoffmann, R.; Yamamoto, A.; Stille, J. K. *Bull. Chem. Soc.* **1981**, *54*, 1857. (b) Yamamoto, A. *Organotransition Metal Chemistry, Fundamental Concepts and Applications*, Wiley-Interscience: New York, 1986; p 286. (c) Brown, J. M.; Cooley, N. A. *Chem. Rev.* **1988**, *88*, 1031.

The activation energy of reductive elimination at the second stage corresponds to the energy difference between the ground state and the transition state. Since, in the reactions of **2a–2d**, all of the [PtR(SiPh₃)-(PhC≡CPh)(PMe₂Ph)] intermediates possess the same ligands except for the alkyl ligands, the stability of ground states may be dependent predominantly upon the Pt–R bond energies, which decrease in the order Pt–Me > Pt–Et > Pt–Pr ≥ Pt–Bu.^{12,13} On the other hand, the relative stability of the transition states will be dependent mainly upon the bond energies of partially formed R–Si bonds. Since Si–Me bond is known to be 7.9 kcal/mol stronger than Si–Et bond,¹⁴ the bond strengths decrease very probably in the order Si–Me >> Si–Et > Si–Pr ≥ Si–Bu. Consequently, the observed reactivity order (**2a** >> **2b** > **2c** ≥ **2d**) toward reductive elimination does not coincide with the expected stability order of the ground states, but agrees with the stability order of the transition states, which is governed mainly by the R–Si bond strengths.

Recent theoretical and thermochemical data have indicated that the Pt–Si bond is much stronger than the Pt–C bond,¹⁵ and this will be one of the reasons for the relatively insensitive nature of ground states, as compared with transition states, to the sorts of alkyl ligands. Furthermore, the marked dependence of reductive elimination rates upon the R–Si bond strengths strongly suggests the reaction mechanism involving a late transition state. This assumption is well in accord with the recent ab initio MO calculation for the C–Si reductive elimination from Pt(CH₃)(SiMe₃)(η²-ethylene)-(PH₃).⁴ Thus, the calculated C–Si bond distance in the transition state (2.042 Å) is closer to that in the product methylsilane (1.923 Å) than that in the ground state (2.889 Å), showing a product-like transition state.

Experimental Section

General Procedure and Materials. All manipulations were carried out under a nitrogen atmosphere using conventional Schlenk techniques. Nitrogen gas was dried by passing through P₂O₅ (Merck, SICAPENT). NMR spectra were recorded on a JEOL JNM-A400 and Varian Mercury 300 spectrometers. Chemical shifts are reported in δ ppm referred to an internal SiMe₄ standard for ¹H and ¹³C NMR and to an external 85% H₃PO₄ standard for ³¹P NMR. Mass spectra were measured using a Shimadzu QP-5000 GC–mass spectrometer (EI, 70 eV, capillary column). GLC analysis was performed with a GL Sciences GC-353 instrument equipped with a FID detector and a capillary column (TC-1, 30 m). THF, Et₂O, and hexane were dried over sodium benzophenone ketyl and distilled prior to use. CH₂Cl₂ and CD₂Cl₂ were dried over CaH₂ and distilled prior to use. Benzene-*d*₆ and toluene-*d*₈ were dried over LiAlH₄, vacuum transferred, and stored under a nitrogen atmosphere. CDCl₃ was purified by passing through a short Al₂O₃ column and stored under a nitrogen atmosphere. PMe₂-Ph was prepared by the reaction of MeMgBr with PCl₂Ph. *trans*- and *cis*-PtR(SiPh₃)(PMe₂Ph)₂ (R = Me (**1a**, **2a**), Et (**1b**, **2b**)) were prepared as previously reported.^{7,8} All other com-

pounds employed in this study were obtained from commercial sources and used without further purification.

Preparation of *cis*-PtR(SiPh₃)(PMe₂Ph)₂ (R = Pr (2c**), Bu (**2d**)).** Complex **2c** was synthesized as follows. To a solution of *trans*-PtCl(SiPh₃)(PMe₂Ph)₂¹⁶ (342 mg, 0.449 mmol) in THF (4 mL) was added a hexane solution of PrLi (2.59 M, 0.69 mL, 1.79 mmol). The solution was stirred for 30 min at room temperature and then cooled to –30 °C. Methanol (0.3 mL) was slowly added, and the mixture was concentrated to dryness by pumping. The resultant white solid was extracted with CH₂Cl₂ and filtered through a short Celite column. The filtrate was concentrated to ca. 1 mL, and Et₂O (3 mL) was carefully layered on the CH₂Cl₂ solution. The solvent layers were allowed to stand at –70 °C overnight, giving colorless crystals of **2c** (241 mg, 69%). Complex **2d** was similarly prepared by using BuLi in place of PrLi (55%).

2c: ¹H NMR (CDCl₃) δ 0.28 (t, ³J_{H–H} = 6.5 Hz, 3H, PtCH₂CH₂CH₃), 1.01 (d, ²J_{P–H} = 7.8 Hz, ³J_{Pt–H} = 20.4 Hz, 6H, PCH₃), ca. 1.1 (m, 4H, PtCH₂CH₂CH₃, the coupling pattern and exact chemical shift were obscured due to overlap with the PCH₃ signals), 1.26 (d, ²J_{P–H} = 7.2 Hz, ³J_{Pt–H} = 15.0 Hz, 6H, PCH₃), 7.17 (m, 9H, Ph), 7.30 (m, 6H, Ph), 7.48 (m, 4H, Ph), 7.67 (m, 6H, Ph). ¹³C{¹H} NMR (CDCl₃): δ 13.6 (d, ¹J_{P–C} = 21 Hz, ²J_{Pt–C} = 8 Hz, PCH₃), 17.1 (dd, ¹J_{P–C} = 28 Hz, ³J_{P–C} = 5 Hz, ²J_{Pt–C} = 30 Hz, PCH₃), 19.6 (d, ³J_{P–C} = 12 Hz, ²J_{Pt–C} = 107 Hz, PtCH₂CH₂CH₃), 21.1 (dd, ²J_{P–C} = 78 and 7 Hz, ¹J_{Pt–C} = 532 Hz, PtCH₂CH₂CH₃), 25.5 (s, PtCH₂CH₂CH₃), 126.6 (s, SiPh), 126.8 (s, SiPh), 128.1 (d, ³J_{P–C} = 9 Hz, PPh), 129.3 (d, ⁴J_{P–C} = 1 Hz, PPh), 129.4 (d, ⁴J_{P–C} = 1 Hz, PPh), 130.8–131.3 (m, PPh), 137.2 (s, ³J_{Pt–C} = 23 Hz, SiPh), 137.9 (d, ³J_{P–C} = 33 Hz, PPh), 140.5 (dd, ¹J_{P–C} = 40 Hz, ³J_{P–C} = 5 Hz, PPh), 145.6 (d, ³J_{P–C} = 8 Hz, ²J_{Pt–C} = 51 Hz, SiPh); ³¹P{¹H} NMR (CDCl₃) δ –12.6 (d, ²J_{P–P} = 18 Hz, ¹J_{Pt–P} = 1783 Hz), –3.9 (d, ²J_{P–P} = 18 Hz, ¹J_{Pt–P} = 1369 Hz, ²J_{Si–P} = 196 Hz). Anal. Calcd for C₃₇H₄₄P₂PtSi: C, 57.43; H, 5.73. Found: C, 57.13; H, 5.71.

2d: ¹H NMR (CDCl₃) δ 0.44 (t, ³J_{H–H} = 7.8 Hz, 3H, PtCH₂CH₂CH₂CH₃), 0.55 (qui, ³J_{H–H} = 7.2 Hz, 2H, PtCH₂CH₂CH₂CH₃), 0.95 (m, 2H, PtCH₂CH₂CH₂CH₃), 1.07 (d, ²J_{P–H} = 8.0 Hz, ³J_{Pt–H} = 20.0 Hz, 6H, PCH₃), ca. 1.1 (m, 2H, PtCH₂CH₂CH₂CH₃, the coupling pattern and the exact chemical shift were obscure due to overlap with the PCH₃ signals), 1.33 (d, ²J_{P–H} = 6.8 Hz, ³J_{Pt–H} = 15.2 Hz, 6H, PCH₃), 7.21 (m, 9H, Ph), 7.36 (m, 6H, Ph), 7.53 (m, 4H, Ph), 7.72 (m, 6H, Ph); ¹³C{¹H} NMR (CDCl₃) δ 13.6 (d, ¹J_{P–C} = 22 Hz, ³J_{P–C} = 3 Hz, ²J_{Pt–C} = 16 Hz, PCH₃), 13.8 (s, PtCH₂CH₂CH₂CH₃), 17.1 (dd, ¹J_{P–C} = 28 Hz, ³J_{P–C} = 3 Hz, ²J_{Pt–C} = 28 Hz, PCH₃), 18.1 (dd, ²J_{P–C} = 79 and 7 Hz, ¹J_{Pt–C} = 530 Hz, PtCH₂CH₂CH₂CH₃), 28.3 (d, ³J_{P–C} = 11 Hz, ²J_{Pt–C} = 98 Hz, PtCH₂CH₂CH₂CH₃), 34.3 (s, PtCH₂CH₂CH₂CH₃), 126.6 (s, SiPh), 126.8 (s, SiPh), 128.1 (d, ³J_{P–C} = 9 Hz, PPh), 129.3 (s, PPh), 129.4 (s, PPh), 130.8–131.2 (m, PPh), 137.2 (s, ³J_{Pt–C} = 23 Hz, SiPh), 137.9 (d, ³J_{P–C} = 35 Hz, PPh), 140.5 (dd, ¹J_{P–C} = 40 Hz, ³J_{P–C} = 4 Hz, PPh), 145.6 (d, ³J_{P–C} = 7 Hz, ²J_{Pt–C} = 51 Hz, SiPh); ³¹P{¹H} NMR (CDCl₃) δ –12.8 (d, ²J_{P–P} = 18 Hz, ¹J_{Pt–P} = 1784 Hz), –4.9 (d, ²J_{P–P} = 18 Hz, ¹J_{Pt–P} = 1367 Hz, ²J_{Si–P} = 196 Hz). Anal. Calcd for C₃₈H₄₆P₂PtSi: C, 57.93; H, 5.88. Found: C, 57.63; H, 5.88.

Preparation of *cis*-PtEt(GePh₃)(PMe₂Ph)₂ (3b**).** *trans*-PtCl(GePh₃)(PMe₂Ph)₂⁷ (249 mg, 0.307 mmol) and EtLi (60 mg, 1.67 mmol) were placed in a Schlenk tube, and THF (4 mL) was added at 0 °C. The mixture was stirred for 30 min at room temperature and then cooled to –30 °C. MeOH (3 mL) was slowly added, and the mixture was concentrated to dryness by pumping. The resulting white solid was extracted with CH₂Cl₂ (3 mL × 2) and filtered through a short Celite column. The filtrate was concentrated to ca. 1 mL. Et₂O (3 mL) was layered on the CH₂Cl₂ solution, and the solvent layers were allowed to stand at –70 °C overnight to give colorless crystals of **3b** (123 mg, 50%).

(13) Simões, J. A. M.; Beauchamp, J. L. *Chem. Rev.* **1990**, *90*, 629.
(14) Pilcher, G.; Skinner, H. A. In *The Chemistry of the Metal–Carbon Bond*, Vol. 1; Hartley, F. R., Patai, S., Eds.; John Wiley: Chichester, 1982; p 43.

(15) (a) Sakaki, S.; Ieki, M. *J. Am. Chem. Soc.* **1991**, *113*, 5063. (b) Sakaki, S.; Ieki, M. *J. Am. Chem. Soc.* **1993**, *115*, 2373. (c) Sakaki, S.; Kai, S.; Sugimoto, M. *Organometallics* **1999**, *18*, 4825. (d) Levy, C. J.; Puddephatt, R. J. *J. Am. Chem. Soc.* **1997**, *119*, 10127. (e) Levy, C. J.; Puddephatt, R. J. *Organometallics* **1997**, *16*, 4115.

(16) Chatt, J.; Eaborn, C.; Ibekwe, S. D.; Kapoor, P. N. *J. Chem. Soc. (A)* **1970**, 1343.

3b: ^1H NMR (CDCl_3) δ 0.77 (q, $^3J_{\text{H-H}} = 7.5$ Hz, $^2J_{\text{Pt-H}} = 55.2$ Hz, 2H, PtCH_2CH_3), 1.16 (d, $^2J_{\text{P-H}} = 7.8$ Hz, $^3J_{\text{Pt-H}} = 19.5$ Hz, 6H, PCH_3), 1.28 (m, 2H, PtCH_2CH_3), 1.40 (d, $^2J_{\text{P-H}} = 7.5$ Hz, $^3J_{\text{Pt-H}} = 21.0$ Hz, 6H, PCH_3), 7.20 (m, 9H, Ph), 7.31 (m, 3H, Ph), 7.36 (m, 3H, Ph), 7.54 (m, 4H, Ph), 7.20 (m, 6H, Ph); $^{13}\text{C}\{^1\text{H}\}$ NMR (CDCl_3) δ 8.7 (dd, $^2J_{\text{P-C}} = 82$ and 7 Hz, $^1J_{\text{Pt-C}} = 503$ Hz, PtCH_2CH_3), 13.8 (dd, $^1J_{\text{P-C}} = 26$ Hz, $^3J_{\text{P-C}} = 3$ Hz, $^2J_{\text{Pt-C}} = 24$ Hz, PCH_3), 16.8 (dd, $^3J_{\text{P-C}} = 5$ and 2 Hz, $^2J_{\text{Pt-C}} = 22$ Hz, PtCH_2CH_3), 17.4 (dd, $^1J_{\text{P-C}} = 28$ Hz, $^3J_{\text{P-C}} = 4$ Hz, $^2J_{\text{Pt-C}} = 25$ Hz, PCH_3), 126.4 (s, GePh), 126.9 (s, GePh), 128.2 (d, $^3J_{\text{P-C}} = 9$ Hz, PPh), 129.5 (d, $^4J_{\text{P-C}} = 2$ Hz, PPh), 129.6 (d, $^4J_{\text{P-C}} = 2$ Hz, PPh), 131.0 (d, $^2J_{\text{P-C}} = 12$ Hz, $^3J_{\text{Pt-C}} = 17$ Hz, PPh), 131.2 (d, $^2J_{\text{P-C}} = 11$ Hz, $^3J_{\text{Pt-C}} = 19$ Hz, PPh), 136.6 (d, $^4J_{\text{P-C}} = 1$ Hz, $^3J_{\text{Pt-C}} = 15$ Hz, GePh), 137.4 (dd, $^1J_{\text{P-C}} = 41$ Hz, $^3J_{\text{P-C}} = 1$ Hz, PPh), 140.0 (dd, $^1J_{\text{P-C}} = 40$ Hz, $^3J_{\text{P-C}} = 3$ Hz, PPh), 148.5 (dd, $^3J_{\text{P-C}} = 10$ and 2 Hz, $^2J_{\text{Pt-C}} = 71$ Hz, GePh); $^{31}\text{P}\{^1\text{H}\}$ NMR (CDCl_3) δ -14.5 (d, $^2J_{\text{P-P}} = 17$ Hz, $^1J_{\text{Pt-P}} = 1699$ Hz), -5.1 (d, $^2J_{\text{P-P}} = 17$ Hz, $^1J_{\text{Pt-P}} = 2048$ Hz). Anal. Calcd for $\text{C}_{36}\text{H}_{42}\text{P}_2\text{PtGe}$: C, 53.76; H, 5.26. Found: C, 53.14; H, 5.09.

X-ray Diffraction Studies. All measurements were performed on a Rigaku AFC7R four-circle diffractometer with graphite-monochromated Mo K α radiation ($\lambda = 0.71069$ Å). Unit cell dimensions were obtained from least-squares treatments of the setting angles of 25 reflections in the range $29.8^\circ < \theta < 30.0^\circ$ for **2c** and of 23 reflections in the range $29.5^\circ < \theta < 30.0^\circ$ for **3b**, respectively. Diffraction data were collected at 23 °C using ω - 2θ scan technique at a scan rate of $16^\circ \text{ min}^{-1}$ in omega.

All calculations were performed with the Texsan Crystal Structure Analysis Package provided by Rigaku Corp., Tokyo. The scattering factors were taken from ref 17. The structures were solved by heavy atom Patterson methods (PATTY) and expanded using Fourier techniques (DIRDIF94). Each structure was refined by full-matrix least-squares with anisotropic thermal parameters for all non-hydrogen atoms. In the final cycles of refinement, hydrogen atoms were located at idealized positions ($d(\text{C-H}) = 0.95$ Å) with isotropic temperature factors ($B_{\text{iso}} = 1.20 B_{\text{bonded atom}}$) and were included in calculation without refinement of their parameters. The function minimized in least-squares was $\sum w(F_o^2 - F_c^2)^2$ ($w = 1/[\sigma^2(F_o^2)]$). Crystal data and details of data collection and refinement are summarized in Table 3. Additional data are available as Supporting Information.

Thermolysis Reactions. A typical procedure for the thermolysis of **2b** is as follows. *cis*-PtEt(SiPh $_3$)(PMe $_2$ Ph) $_2$ (**2b**) (9.35 mg, 12.3 μmol), diphenylacetylene (21.4 mg, 0.120 mmol), and MeSiPh $_3$ (3.02 mg, 11.0 μmol) as an internal standard for GLC analysis were placed in an NMR sample tube equipped with a rubber septum cap. The system was replaced with nitrogen gas at room temperature, and benzene (0.6 mL) was added. The resulting colorless solution was heated at 40 °C using an oil bath, and the reaction progress was monitored at intervals by $^{31}\text{P}\{^1\text{H}\}$ NMR spectroscopy at room temperature. After the reaction was completed, the solution was analyzed by GLC and GC-mass spectrometry, showing the formation of EtSiPh $_3$ in 98% yield.

Preparation and Thermolysis of *cis*-Pt(CH $_2$ CD $_3$)(SiPh $_3$)(PMe $_2$ Ph) $_2$ (2b-d $_3$**).** To a Schlenk tube were added *trans*-PtCl(SiPh $_3$)(PMe $_2$ Ph) $_2$ (200 mg, 0.263 mmol) and CD $_3$ CH $_2$ Li (46 mg, 1.18 mmol), which was prepared by the reaction of Li metal and CD $_3$ CH $_2$ Br (99% isotopic purity) 18 in pentane under reflux. THF (3.5 mL) was added at 0 °C, and the mixture was stirred at room temperature for 30 min. MeOH (3 mL) was slowly added, and the mixture was concentrated to dryness by pumping. The resulting white solid was extracted with CH $_2$ -Cl $_2$ (3 mL \times 2) and filtered through a short Celite column.

Table 3. Crystal Data and Details of the Structure Determination of **2c and **3b****

	2c	3b
formula	$\text{C}_{37}\text{H}_{44}\text{P}_2\text{SiPt}$	$\text{C}_{36}\text{H}_{42}\text{P}_2\text{GePt}$
fw	773.88	804.36
cryst size, mm	$0.32 \times 0.20 \times 0.16$	$0.25 \times 0.20 \times 0.18$
color/shape	colorless/prism	colorless/prism
cryst syst	monoclinic	triclinic
space group	$P2_1$ (No. 4)	$P\bar{1}$ (No. 2)
<i>a</i> , Å	11.130(2)	10.549(3)
<i>b</i> , Å	9.315(3)	19.195(4)
<i>c</i> , Å	17.426(2)	8.920(2)
α , deg	89.44(2)	
β , deg	106.17(1)	108.93(2)
γ , deg	97.85(2)	
<i>V</i> , Å 3	1735.1(6)	1691.4(8)
<i>Z</i>	2	2
d_{calcd} , g cm $^{-3}$	1.481	1.579
$\mu(\text{Mo K}\alpha)$, cm $^{-1}$	41.78	51.20
<i>F</i> (000)	776	796
radiation	Mo K α ($\lambda = 0.71069$ Å)	Mo K α ($\lambda = 0.71069$ Å)
monochromator	graphite	graphite
data collected	$+h, +k, \pm l$	$+h, \pm k, \pm l$
2θ max, deg	55.0	55.1
scan type	ω - 2θ	ω - 2θ
$\Delta\omega$, deg	$1.26 + 0.30 \tan \theta$	$1.89 + 0.35 \tan \theta$
scan speed, deg min $^{-1}$	16, fixed	16, fixed
temp, K	293	293
linear decay, %	3.93	10.97
abs corr	empirical	empirical
min and max	0.473, 0.999	0.485, 0.999
transm factors		
no. of reflns collected	4431	8138
no. of unique reflns	4220 ($R_{\text{int}} = 0.067$)	7725 ($R_{\text{int}} = 0.020$)
no. of obsd reflns	3992	7028
($I \geq 3\sigma(I)$)		
no. of variables	370	362
<i>R</i> indices	$R1 = 0.035$ $R = 0.067$ $R_w = 0.102$ GOF = 1.03	$R1 = 0.056$ $R = 0.090$ $R_w = 0.201$ GOF = 1.40
<i>R</i> indices (all data) a	$R1 = 0.035$ $R_w = 0.104$	$R1 = 0.059$ $R_w = 0.245$
max Δ/σ in final cycle	0.001	0.001
max and min	2.50, -2.79	4.16, -3.59
peak, e Å $^{-3}$	(near Pt)	(near Pt)

a Function minimized = $\sum w(F_o^2 - F_c^2)^2$; $w = 1/[\sigma^2(F_o^2)]$. $R1 = \sum ||F_o| - |F_c|| / \sum |F_o|$. $R = \sum (F_o^2 - F_c^2) / \sum (F_o^2)$. $R_w = [\sum w(F_o^2 - F_c^2)^2 / \sum w(F_o^2)^2]^{1/2}$. GOF = $[\sum w(|F_o| - |F_c|)^2 / (N_o - N_v)]^{1/2}$, where N_o is the number of observations and N_v the number of variables.

The filtrate was concentrated to ca. 1 mL, and Et $_2$ O (4 mL) was layered on the CH $_2$ Cl $_2$ solution. The solvent layers were allowed to stand at -70 °C overnight to give colorless crystals of **2b-d $_3$** (138 mg, 69%). The ^1H NMR spectrum measured in CD $_2$ Cl $_2$ at -20 °C was identical with **2b** except for the absence of the PtCH $_2$ CH $_3$ signal at δ 0.65. 8,19

Complex **2b-d $_3$** (10.0 mg, 13.1 μmol) and diphenylacetylene (23.0 mg, 0.129 mmol) were placed in an NMR sample tube and dissolved in benzene- d_6 (0.60 mL) at room temperature. The mixture was heated at 40 °C overnight. ^2D NMR spectra of the resulting solution exhibited the signals arising from methyl and methylene protons of EtSiPh $_3$ (δ 1.09 and 1.28, respectively) in a 3.1:1.9 ratio.

Kinetic Studies on the Thermolysis of **2b-**2d**.** *cis*-PtEt(SiPh $_3$)(PMe $_2$ Ph) $_2$ (**2b**) (10.64 mg, 14.0 μmol), diphenylacetylene (24.95 mg, 0.140 mmol), and 4,4'-dimethylbiphenyl (1.28 mg, 7.0 μmol) were placed in an NMR sample tube equipped with

(17) Cromer, D. T.; Waber, J. T. *International Tables for X-ray Crystallography*; The Kynoch Press: Birmingham, U.K., 1974; Vol. IV.

(18) Yamamoto, T.; Saruyama, T.; Nakamura, Y.; Yamamoto, A. *Bull. Chem. Soc. Jpn.* **1976**, *49*, 589.

(19) In the previous report, 8 we assigned the signal at δ 0.65 to the methylene protons of the PtEt group. However, the ^1H NMR spectrum of **2b-d $_3$** revealed that the signal was arising from the methyl protons, not from the methylene protons. The methylene proton signal was overlapped with the PMe signal at δ 1.05 in CD $_2$ Cl $_2$, but clearly observed at δ 1.72, separating from the PMe signal, in benzene- d_6 .

a rubber septum cap, and the system was replaced with nitrogen gas at room temperature. Benzene-*d*₆ was added to adjust total volume of the solution to 0.70 mL. The sample tube was placed in an NMR sample probe controlled to 50.0 ± 0.1 °C, and the thermolysis reaction was followed by ¹H NMR spectroscopy. The amounts of **2b**, *cis*-PtPh(SiEtPh₂)(PMe₂Ph)₂ (**5b**), and Pt(PhC≡CPh)(PMe₂Ph)₂ (**6**) at intervals were determined by measuring relative peak integration of the methyl signal of 4,4'-dimethylbiphenyl (δ 2.15), the methylene signal of **2b** (δ 1.72 (m)), the PMe signal of **5b** (δ 0.72 (d)), and the PMe signal of **6** (δ 1.48 (d)). The relative amounts of the platinum complexes were confirmed also by ³¹P{¹H} NMR spectroscopy: **2b** [δ -5.3 (d, ²J_{P-P} = 18 Hz, ¹J_{Pt-P} = 1369 Hz), -12.8 (d, ²J_{P-P} = 18 Hz, ¹J_{Pt-P} = 1773 Hz)], **5b** [δ -6.4 (d, ²J_{P-P} = 19 Hz, ¹J_{Pt-P} = 1133 Hz), -14.4 (d, ²J_{P-P} = 19 Hz, ¹J_{Pt-P} = 1953 Hz)], **6** [δ -13.2 (s, ¹J_{Pt-P} = 3305 Hz)].

The thermolysis reactions of **2c** and **2d** were followed by ³¹P{¹H} NMR spectroscopy. A typical spectrum for **2c** is given in Figure 3, together with the NMR data of **2c**, **5c**, and **6**. The data of **2d** and **5d** in the thermolysis solution (benzene-*d*₆, 55 °C) are as follows: **2d** [δ -5.5 (d, ²J_{P-P} = 19 Hz, ¹J_{Pt-P} = 1324 Hz), -12.8 (d, ²J_{P-P} = 19 Hz, ¹J_{Pt-P} = 1778 Hz)], **5d** [δ -6.7 (d, ²J_{P-P} = 18 Hz, ¹J_{Pt-P} = 1130 Hz), -14.6 (d, ²J_{P-P} = 18 Hz, ¹J_{Pt-P} = 1950 Hz)].

Preparation and Identification of *cis*-PtPh(SiRPh₂)(PMe₂Ph)₂. The *cis*-phenyl-silyl complexes bearing SiMePh₂ and SiPh₃ ligands (**5a** and **5e**, respectively) were prepared by isomerization of the corresponding trans isomers (**4a** and **4e**, respectively) promoted by carbon monoxide in solution.

(a) Preparation of **4a and **4e**.** The complex *trans*-PtCl(SiMePh₂)(PMe₂Ph)₂¹⁶ (504 mg, 0.72 mmol) was placed in a Schlenk tube and dissolved in THF (7 mL) at room temperature. The solution was cooled to -30 °C, and an Et₂O solution of PhLi (1.8 M, 0.44 mL, 0.79 mmol) was added. After stirring for 30 min at the same temperature, MeOH (0.1 mL) was added, and the mixture was concentrated to dryness to give a white solid, which was extracted with CH₂Cl₂ (3 mL × 3) at room temperature, filtered through a filter-paper-tipped cannula, and then concentrated to dryness. The resulting solid of *trans*-PtPh(SiMePh₂)(PMe₂Ph)₂ (**4a**) was washed with a 2:5 mixture of Et₂O and hexane (7 mL × 2) and dried under vacuum (350 mg, 66%). Similarly, *trans*-PtPh(SiPh₃)(PMe₂Ph)₂ (**4e**) was obtained in 55% yield from *trans*-PtCl(SiPh₃)(PMe₂Ph)₂.¹⁶

4a: ¹H NMR (CD₂Cl₂) δ 0.29 (s, ³J_{Pt-H} = 14.8 Hz, 3H, SiCH₃), 1.18 (virtual triplet, *J* = 3.6 Hz, ³J_{Pt-H} = 32.0 Hz, 12H, PCH₃), 6.71 (t, 1H, Ph), 6.86 (t, 2H, Ph), 7.09 (d, 2H, Ph), 7.10 (d, 4H, Ph), 7.17 (d, ³J_{Pt-H} = 31.2 Hz, 2H, Ph), 7.26–7.50 (m, 14H, Ph). ¹³C{¹H} NMR (CD₂Cl₂): δ 4.5 (s, ²J_{Pt-C} = 36 Hz, SiCH₃), 15.9 (virtual triplet, *J* = 20 Hz, ²J_{Pt-C} = 40 Hz, PCH₃), 122.0 (s, PtPh), 126.7 (s, SiPh), 127.1 (s, SiPh), 127.3 (s, ²J_{Pt-C} = 40 Hz, PtPh), 128.3 (virtual triplet, *J* = 5 Hz, PPh), 129.8 (s, PPh), 131.6 (virtual triplet, *J* = 6 Hz, ³J_{Pt-C} = 25 Hz, PPh), 135.9 (s, ³J_{Pt-C} = 12 Hz, SiPh), 137.0 (virtual triplet, *J* = 28 Hz, ²J_{Pt-C} = 33 Hz, PPh), 139.8 (s, ³J_{Pt-C} = 20 Hz, PtPh), 150.3 (s, ²J_{Pt-C} = 26 Hz, SiPh), 172.5 (t, ²J_{P-C} = 13 Hz, ¹J_{Pt-C} = 527 Hz, PtPh); ³¹P{¹H} NMR (CD₂Cl₂) δ -7.5 (s, ¹J_{Pt-P} = 2793 Hz). Anal. Calcd for C₃₅H₄₀SiP₂Pt: C, 56.37; H, 5.41. Found: C, 56.44; H, 5.47.

4e: ¹H NMR (CD₂Cl₂) δ 1.08 (virtual triplet, *J* = 3.4 Hz, ³J_{Pt-H} = 32.2 Hz, 12H, PCH₃), 6.69 (t, *J* = 7.3 Hz, 1H, Ph), 6.80 (t, *J* = 7.3 Hz, 2H, Ph), 7.04–7.30 (m, 21H, Ph), 7.52 (m, 6H, Ph); ¹³C{¹H} NMR (CD₂Cl₂) δ 15.3 (virtual triplet, *J* = 20 Hz, ²J_{Pt-C} = 40 Hz, PCH₃), 122.1 (s, PtPh), 127.0 (s, SiPh), 127.1 (s, SiPh), 127.3 (s, ²J_{Pt-C} = 40 Hz, PtPh), 128.1 (virtual triplet, *J* = 5 Hz, PPh), 129.5 (s, PPh), 131.4 (virtual triplet, *J* = 7 Hz, ³J_{Pt-C} = 26 Hz, PPh), 136.6 (t, ²J_{P-C} = 29 Hz, PtPh), 137.4 (s, ²J_{Pt-C} = 15 Hz, SiPh), 140.0 (s, ³J_{Pt-C} = 15 Hz, PtPh), 147.9 (s, ²J_{Pt-C} = 28 Hz, SiPh), 170.9 (t, *J* = 13 Hz, PtPh); ³¹P{¹H} NMR (CD₂Cl₂) δ -9.2 (s, ¹J_{Pt-P} = 2756 Hz). Anal.

Calcd for C₄₀H₄₂SiP₂Pt: C, 59.47; H, 5.24. Found: C, 59.20; H, 5.09.

(b) Preparation of **5a and **5e**.** Complex **4a** (250 mg, 0.34 mL) was placed in a Schlenk tube and dissolved in CH₂Cl₂ (3 mL) at room temperature. The solution was cooled to -30 °C, and CO gas was bubbled for 1 h with stirring. The ³¹P{¹H} NMR spectrum showed complete conversion of **4a** to *cis*-PtPh(SiMePh₂)(PMe₂Ph)₂ (**5a**). The solution was concentrated to dryness, and the resulting white solid was washed with hexane (3 mL × 2) and dried under vacuum (208 mg, 83%). The conversion of **4e** to **5e** was similarly conducted. The isomerization was complete after 4 h at -20 °C, and **5e** was isolated as a white solid in 97% yield.

5a: ¹H NMR (CD₂Cl₂, -20 °C) δ -0.24 (s, ³J_{Pt-H} = 25.8 Hz, 3H, SiCH₃), 0.94 (d, ²J_{P-H} = 7.6 Hz, ³J_{Pt-H} = 16.8 Hz, 6H, PCH₃), 1.03 (d, ²J_{P-H} = 8.4 Hz, ³J_{Pt-H} = 22.4 Hz, 6H, PCH₃), 6.67 (brt, 1H, Ph), 6.85 (brt, 2H, Ph), 7.14–7.44 (m, 18H, Ph), 7.70 (d, 4H, Ph); ¹³C{¹H} NMR (CD₂Cl₂, -20 °C) δ 4.8 (s, ²J_{Pt-C} = 66 Hz, SiCH₃), 13.3 (d, ¹J_{P-C} = 26 Hz, ²J_{Pt-C} = 23 Hz, PCH₃), 16.4 (d, ¹J_{P-C} = 31 Hz, ³J_{P-C} = 5 Hz, ²J_{Pt-C} = 30 Hz, PCH₃), 120.9 (s, PtPh), 127.0 (s, SiPh), 127.0 (s, PtPh), 127.3 (s, SiPh), 128.2 (d, ³J_{P-C} = 8 Hz, PPh), 128.3 (d, ³J_{P-C} = 8 Hz, PPh), 129.3 (s, PPh), 129.6 (s, PPh), 130.7 (d, ²J_{P-C} = 12 Hz, PPh), 130.9 (d, ²J_{P-C} = 12 Hz, PPh), 137.6 (d, ¹J_{P-C} = 33 Hz, PPh), 138.6 (s, ³J_{Pt-C} = 40 Hz, PtPh), 139.0 (dd, ¹J_{P-C} = 42 Hz, ³J_{P-C} = 3 Hz, ²J_{Pt-C} = 46 Hz, PPh), 147.8 (dd, ³J_{P-C} = 8 and 3 Hz, ²J_{Pt-C} = 49 Hz, SiPh), 161.3 (dd, ²J_{P-C} = 97 and 13 Hz, ¹J_{Pt-C} = 720 Hz, PtPh); ³¹P{¹H} NMR (CD₂Cl₂, -20 °C) δ -5.6 (d, ²J_{P-P} = 19 Hz, ¹J_{Pt-P} = 1240 Hz, ²J_{Si-P} = 178 Hz), -14.8 (d, ²J_{P-P} = 19 Hz, ¹J_{Pt-P} = 1936 Hz). Anal. Calcd for C₃₅H₄₀SiP₂Pt: C, 56.37; H, 5.41. Found: C, 56.17; H, 5.45.

5e: ¹H NMR (CD₂Cl₂) δ 0.91 (d, ²J_{P-H} = 7.8 Hz, ³J_{Pt-H} = 16.6 Hz, 6H, PCH₃), 1.03 (d, ²J_{P-H} = 8.3 Hz, ³J_{Pt-H} = 22.0 Hz, 6H, PCH₃), 6.36 (brt, 1H, Ph), 6.47 (brt, 2H, Ph), 6.96 (brt, 2H, Ph), 7.05–7.40 (m, 19H, Ph), 7.53 (m, 6H, Ph); ¹³C{¹H} NMR (CD₂Cl₂) δ 13.4 (d, ¹J_{P-C} = 25 Hz, ²J_{Pt-C} = 23 Hz, PCH₃), 16.6 (d, ¹J_{P-C} = 30 Hz, ²J_{Pt-C} = 30 Hz, ³J_{P-C} = 5 Hz, PCH₃), 120.7 (d, ⁵J_{P-C} = 3 Hz, PtPh), 126.9 (s, SiPh), 127.1 (dd, ³J_{P-C} = 4 and 2 Hz, ²J_{Pt-C} = 59 Hz, PtPh), 128.4 (d, ³J_{P-C} = 10 Hz, PPh), 128.7 (d, ³J_{P-C} = 9 Hz, PPh), 129.4 (s, PPh), 120.0 (s, PPh), 131.0 (d, ²J_{P-C} = 10 Hz, ³J_{Pt-C} = 9 Hz, PPh), 131.4 (d, ²J_{P-C} = 12 Hz, ³J_{Pt-C} = 17 Hz, PPh), 137.2 (s, ³J_{Pt-C} = 22 Hz, SiPh), 137.6 (dd, ²J_{P-C} = 38 Hz, ⁴J_{P-C} = 3 Hz, PPh), 138.9 (d, ⁴J_{P-C} = 2 Hz, ³J_{Pt-C} = 36 Hz, PtPh), 139.6 (dd, ²J_{P-C} = 41 Hz, ⁴J_{P-C} = 2 Hz, PPh), 145.8 (dd, ²J_{Pt-C} = 52 Hz, ³J_{P-C} = 6 and 2 Hz, SiPh), 159.0 (dd, ²J_{P-C} = 101 and 14 Hz, PtPh); ³¹P{¹H} NMR (CD₂Cl₂) δ -4.2 (d, ²J_{P-P} = 19 Hz, ¹J_{Pt-P} = 1156 Hz, ²J_{Si-P} = 183 Hz), -13.4 (d, ²J_{P-P} = 19 Hz, ¹J_{Pt-P} = 1808 Hz). Anal. Calcd for C₄₀H₄₂SiP₂Pt: C, 59.47; H, 5.24. Found: C, 59.41; H, 5.04.

(c) Identification of **5b–**5d**.** A typical example is as follows. Complex **2d** (15.0 mg, 19.0 mmol) was placed in an NMR sample tube and dissolved in CD₂Cl₂ (0.6 mL) under a nitrogen atmosphere. The sample was allowed to stand at room temperature and examined by ³¹P{¹H} NMR spectroscopy at intervals. After 2 days, about 84% of **2d** was converted into **5d**. In addition, two singlets arising from unidentified species were observed at δ -4.8 and -21.2. The NMR data of **5b**–**5d** are as follows.

5b: ¹H NMR (CDCl₃) δ 0.42 (q, ³J_{H-H} = 7.6 Hz, 2H, SiCH₂CH₃), 0.55 (t, ³J_{H-H} = 8.0 Hz, 3H, SiCH₂CH₃), 0.90 (d, ²J_{P-H} = 7.2 Hz, ³J_{Pt-H} = 15.6 Hz, 6H, PCH₃), 1.00 (d, ²J_{P-H} = 8.4 Hz, ³J_{Pt-H} = 19.2 Hz, 6H, PCH₃), 6.72 (brt, 1H, Ph), 6.88 (brt, 2H, Ph), 7.15–7.60 (m, 18H, Ph), 7.81 (m, 4H, Ph); ³¹P{¹H} NMR (CDCl₃) δ -6.1 (d, ²J_{P-P} = 19 Hz, ¹J_{Pt-P} = 1160 Hz, ²J_{Si-P} = 174 Hz), -14.6 (d, ²J_{P-P} = 19 Hz, ¹J_{Pt-P} = 1948 Hz).

5c: ¹H NMR (CD₂Cl₂) δ 0.42 (m, 2H, SiCH₂CH₂CH₃), 0.58 (t, ³J_{H-H} = 7.2 Hz, 3H, SiCH₂CH₂CH₃), 0.91 (d, ²J_{P-H} = 7.6 Hz, ³J_{Pt-H} = 16.0 Hz, 6H, PCH₃), 1.04 (d, ²J_{P-H} = 8.0 Hz, ³J_{Pt-H} = 22.4 Hz, 6H, PCH₃), 1.42 (m, 2H, SiCH₂CH₂CH₃), 6.68 (brt, 1H, Ph), 6.84 (brt, 2H, Ph), 7.16–7.65 (m, 18H, Ph), 7.75 (m,

4H, Ph); $^{31}\text{P}\{^1\text{H}\}$ NMR (CD_2Cl_2) δ -6.1 (d, $^2J_{\text{P-P}} = 19$ Hz, $^1J_{\text{Pt-P}} = 1188$ Hz, $^2J_{\text{Si-P}} = 182$ Hz), -14.8 (d, $^2J_{\text{P-P}} = 19$ Hz, $^1J_{\text{Pt-P}} = 1949$ Hz).

5d: ^1H NMR (CD_2Cl_2) δ 0.45 (m, 2H, $\text{SiCH}_2\text{CH}_2\text{CH}_2\text{CH}_3$), 0.63 (brt, 3H, $\text{SiCH}_2\text{CH}_2\text{CH}_2\text{CH}_3$), 0.91 (d, $^2J_{\text{P-H}} = 7.6$ Hz, $^3J_{\text{Pt-H}} = 17.6$ Hz, 6H, PCH_3), 1.03 (d, $^2J_{\text{P-H}} = 8.4$ Hz, $^3J_{\text{Pt-H}} = 21.6$ Hz, 6H, PCH_3), 1.41 (m, 4H, $\text{SiCH}_2\text{CH}_2\text{CH}_2\text{CH}_3$), 6.67 (brt, 1H, Ph), 6.82 (brt, 2H, Ph), 7.10–7.55 (m, 18H, Ph), 7.75 (d, 4H, Ph); $^{31}\text{P}\{^1\text{H}\}$ NMR (CD_2Cl_2) δ -6.2 (d, $^2J_{\text{P-P}} = 18$ Hz, $^1J_{\text{Pt-P}} = 1184$ Hz, $^2J_{\text{Si-P}} = 182$ Hz), -14.8 (d, $^2J_{\text{P-P}} = 18$ Hz, $^1J_{\text{Pt-P}} = 1949$ Hz).

Acknowledgment. This work was supported by a Grant-in-Aid for Scientific Research on Priority Area

“The Chemistry of Inter-element Linkage” (No. 09239105) from the Ministry of Education, Science, Sports and Culture, Japan.

Supporting Information Available: Details of the structure determination of **2c** and **3b** including figures giving atomic numbering schemes and tables of atomic coordinates, thermal parameters, and full bond distances and angles. This material is available free of charge via the Internet at <http://pubs.acs.org>.

OM000012T